Journal of Computational Applied Mechanics 2020, 52(1)
DOI: 10.22059/jcamech.2021.319378.601

RESEARCH PAPER

A review on the mechanics of inertial microfluidics

Daniyal Farajpour*

Department of Mechanical Engineering, School of Engineering, Vali-e-Asr University of Rafsanjan, Iran

Abstract
In a number of microfluidics-based systems where the Reynolds number is in an intermediate range, both viscosity and inertia are significant, and thus, plenty of interesting effects appear including inertial motion and secondary flow. In recent years, this rapidly expanding area of science has opened new window of possibilities for micro-particle inertial focusing in high-throughput cellular separation and physiological fluids processing. Moreover, this science is applicable in bio-particle focusing in clinical diagnostics along with widespread applications in environmental cleanup. In this review, fundamental concepts governing the mechanics and physics of inertial microfluidics are discussed. Furthermore, recent mathematical frameworks and theoretical developments that have made this science what we know today are presented in detail. Finally, a number of possible futuristic promising directions in this novel field are proposed since despite tremendous recent progress, this mainstream technology is still a nascent area of research.
Keywords: Microfluidics, Inertial terms, Microchannels, Ultrasmall particles, Cell isolation.

Introduction

Nanotechnology and microtechnology are expected to change our world in the near future, and bring many useful devices and systems that would make our lives much easier [1-5]. A number of novel nanomaterials [6-9] and small-scale structures [10-13] have been synthesised, which have shown excellent mechanical and electrical properties [14-16]. Moreover, various ultrasmall electromechanical systems such as microfluidic devices [17, 18], mass sensors [19] and resonators [20] have been introduced with promising applications. In microfluidics [21-23], the behavior of a particle flowing in a microchannel is precisely studied as well as methods to control and manipulate a particle in micro-channels have also being investigated [17]. Take inertial focusing as a good example of manipulation of a micro-particle transported by a fluid in micro-channels [24]; through which the particle's motion can be well controlled [25]. This technology is advantageous in comparison with other microscale platforms mainly because the motion of the particle is governed by its inherent hydrodynamic forces [26] and those non-hydrodynamic forces mostly are not needed [27]. Moreover, there are other advantages such as: fast sample processing, low cost, reduced sample and reagent volumes, high sensitivity, and finally the potential to be automated for the sake of reducing human intervention and its subsequent inevitable errors [28]. Therefore, this science has several applications in various fields ranging from biology to biomedicine [29, 30].
Lateral motion and focusing of particles were firstly observed in a cylindrical pipe experiment by Segre and Silberberg in 1960s [31]. Microfluidic technologies, however, came into the picture decades later studying particles behavior in micro-channels. Then, the emergence of inertial focusing in microfluidics captured significant attention since 2007, mainly because of precise particle control by using merely hydrodynamic interactions at relatively high speed

* Corresponding author e-mail: Daniyalfarajpour@gmail.com

[32]. There are plenty of passive and active microfluidics techniques in order to separate cells. Using passive technologies, cells are separated and manipulated without the intervention of any externally applied factors. Hydrophoresis [33], gravitational methods, and deterministic lateral displacement are three of most important examples of the passive techniques [34-36]. Nonetheless, active techniques are field-flow-fractionation techniques (FFF) [37, 38] in which suspended micro-particles are migrating at almost uniform velocities while an external field is applied. Therefore, cells will be separated based on their size or other properties [39, 40]. These active microfluidic techniques include dielectrophoresis, acoustophoresis, and magnetoohoresis [41-45].

Intuitively, inertia in microfluidics had always been considered negligible. As H, microchannel dimensions, is small, therefore, Reynolds number ($\mathrm{Re} = \rho UH / \mu$), a dimensionless parameter defined to describe the ratio between inertia in a flow and its viscosity, would expected to be low in conventional microfluidics. Thus, using Stokes flow was acceptable. However, there are some undeniable cases like water in which this assumption turned out to be fallacious and Reynolds number cannot be considered zero any more [46, 47]. Therefore, Stokes flow cannot be the case. With regard to this condition, intermediate Reynolds number ($\sim 1 < \mathrm{Re} < \sim 100$), both fluid viscosity and inertial should be considered finite. These considerations will result in two major effects in microfluidics (1) inertial migration of particles and (2) secondary flows mostly in curved channels [48].

In this review, we will firstly come up with fundamentals of a suspended particle in a micro-channel. Apparently, this can provide a wider insight of this science helpful in a better understanding. Then, the recent progress in inertial migration has been reviewed. This review will be based on the structure of a micro-channel since it can play a significant role in manipulating and separating micro-particles. Different channel structures have various applications in microfluidic devices according to their intrinsic properties. At the end of the day, the inertial migration future in microfluidics will be discussed and suggestions will be proposed. Hopefully, this study can be aspirational for novices and expand the horizon of more experienced researchers in this area

Physics of a suspended particle in microfluidic channels

There are several forces either drag or lift ones applied on particles moving in a microchannel [49-52]. They are induced by shear and normal stresses acting over particles. Drag forces are parallel while lift ones are at the right angles to the direction of main flow. Some of them play a significant part in physics of these particles while others are often considered negligible and sometimes are less investigated thus remained unknown.

Viscous drag force

An object moving through a fluid tends to displace the fluid elements out of its way. This creates a drag force which is defined for a spherical particle as:

$$F_{drag} = \frac{1}{4} f_{drag} \pi d^2, \tag{1}$$

where d represents the particle diameter, and f_{drag} refers to viscous drag coefficient. The coefficient can be determined by the particle Reynolds number which is defined as:

$$\mathrm{Re}' = \frac{\rho u_t d}{\mu}, \tag{2}$$

where u_t represents the relative velocity of fluid to particle [53]. Because of various range of Reynolds numbers, viscous drag coefficient of a particle [54] can be varied:

If $10^{-4} < \mathrm{Re}' < 0.2$

$$f_{drag} = \frac{12\mu u_t}{d}, \tag{3}$$

Thus

$$F_{drag} = 3\mu u_t \pi d, \tag{4}$$

According to the Reynolds number this formula is known as the Stokes drag which is advantageous because it is simple in the case fluid relative speed, u_t , is low. Therefore it can be frequently used.

If $0.2 < \mathrm{Re}' < 500 \sim 1000$

$$f_{drag} = \frac{12\mu u_t}{d}(0.15\,\mathrm{Re}'^{0.687} + 1), \tag{5}$$

Thus

$$F_{drag} = 3\mu u_t \pi d(0.15\,\mathrm{Re}'^{0.687} + 1), \tag{6}$$

If $500 \sim 1000 < \mathrm{Re}' < 2 \times 10^5$

$$f_{drag} = 0.22\rho_f u_t^{\,2}, \tag{7}$$

Thus

$$F_{drag} = 0.055\rho_f u_t^{\,2} \pi d^2, \tag{8}$$

Two components of this drag force, along mainstream direction and cross-section, are caused by the discrepancies of the longitudinal velocities between particles and fluid in which they are suspended and secondary flow caused by channel curvatures [55] or disturbance structures, respectively.

Physics of inertial migration

In 1960s, Segre and Silberberg showed rigid particle migration induced by lift forces in macroscale flows [31]. The forces indiscriminately dispersed some small particles in a 1 cm pipe then particles were observed to migrate to an annulus-like position that its center is located at a distance which is about 0.6 times greater than the pipe radius (Figure 1). If the inertia is considerable when the Reynolds number is fairly finite, analytical calculations are difficult to obtain, so this phenomenon cannot be justified. Following Segre and Silberberg, efforts increasingly were put into investigating and explaining this phenomenon. By developing our understanding of particle motion and lift forces, precisely manipulating cells and particles will be achievable [56, 57]. Some fundamental external factors including the aspect ratio, channel dimensions, particle diameters, and flow rate are important to control the direction and magnitude of lift forces [58]. While in case of inertial migration there are plenty of forces, two lift forces have been considered dominant and others have often been regarded of negligible values. These two are wall-induced lift force and shear gradient lift force [59]. These important factors are precisely explained in the following sections.

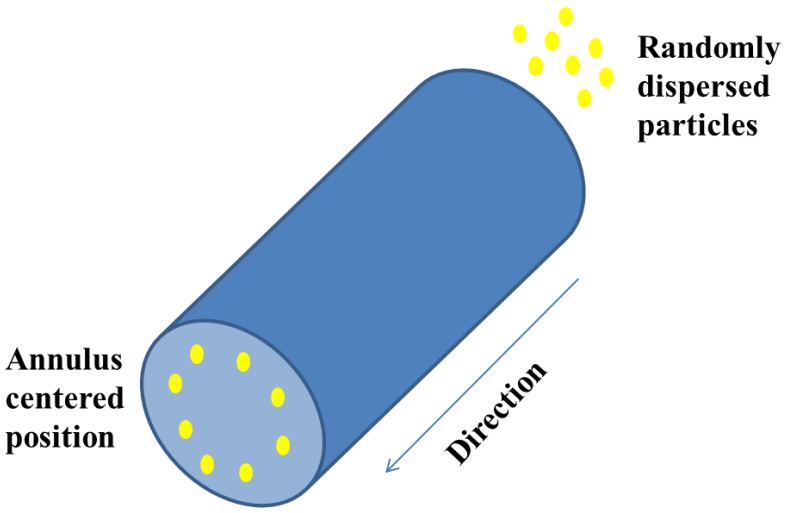

Figure 1. Small particles with a random distribution are gradually located at an annulus after a distance along the flow direction.

Shear gradient lift forces

Apparently because of some wall effects [60] there is a delay between the particle and the flow. According to the parabolic fluid velocity profile, because of the curvature the magnitude of relative fluid to particle velocity is by far greater on the wall side of the particle in comparison to the opposite side (Figure 2). A shear gradient lift force, therefore, is caused by the lower pressure on the wall side. This lift force pushes these particles towards the wall until the wall-induced lift force which will be discussed in the following section balances it. Therefore, an equilibrium position will be resulted [61, 62]. Furthermore, it is interesting that in the linear fluid velocity profile, the values of the relative velocity is lower on the wall side of the particle since there is not a curvature anymore (Figure 2). Thus, the pressure is higher on this side and the direction of this lift force will be towards the channel centerline [63, 64].

Wall-induced lift force

Generally, there are two separate interactions between a wall and a suspended object; First of all, when the particle diameter is much less than the dimension of the channel, nearest wall on one side of the object primarily influences on that object while the effects of other walls are negligible because of their relatively long distances. The particles are pushed away by wall-induced forces, and even its motion is decelerated (Figure 2). Secondly, in a bounded flow, when the particle diameter is of the order of the channel dimension all walls considerably decelerate the motion of the particle [65].
Now, the conditions where the dimensions of particles are too smaller than that of a channel would be discussed. Particles influenced by boundaries can move parallel or perpendicular to the channel walls. In case of perpendicular motion, the wall effects would retard an immersed particle which is directly related to the drag coefficient increase. In the creeping flow moving, a first-order correction for the drag coefficient was derived by Brenner [66].

$$f_{drag} = 16 f \frac{\mu u_t}{d}, \tag{9}$$

$$f = \sinh\theta_w \sum_{n=1}^{\infty} \frac{n(n+1)}{(2n+3)(2n-1)} \times \left[\frac{2\sinh[(2n+1)\sinh 2\theta_w + (2n+1)\theta_w]}{4\sinh^2[\theta_w(n+0.5)] - (2n-1)^2 \sinh^2\theta_w} - 1 \right], \tag{10}$$

$$\theta_w = \cosh^{-1}(\frac{2l_w}{d}), \tag{11}$$

where θ_w is considered a function of l_w to the particle diameter, l_w is defined as sphere distance center to the channel wall (Figure 2a). According to Equation (10), approaching the wall considerably increases the hydrodynamic forces on flowing particles.
Lateral lift forces push the objects away from the wall while the immersed object is moving parallel to the wall. A dimensionless distance is expressed as [67, 68]:

$$d^* = \frac{\rho_f u_s l_w}{\mu}, \tag{12}$$

If $d^* \ll 1$

$$u_z = \frac{3\mathrm{Re}_s u_s}{64}\left[1 - \frac{11}{32}d^{*2} + ...\right], \tag{13}$$

where u_z is the lateral migration velocity as well as u_s is the sedimentation velocity of the sphere in stagnant fluid, therefore Res can be expressed as:

$$\mathrm{Re}_s = \frac{\rho_f u_s d}{\mu}, \tag{14}$$

when $d^* \ll 1$, equation (13) can be more simplified as:

$$u_z = \frac{3\mathrm{Re}_s u_s}{64}, \tag{15}$$

According to equation (15), a sphere moves with a constant migration velocity close to the walls. This claim have been empirically confirmed by the data of Cherukat and McLaughlin [69] up to Re_s=3. On the other hand when $d^* \gg 1$ the migration velocity can be written as:

$$u_z = \frac{3\mathrm{Re}_s u_s}{16}(d^{*-2} + 2.21901 d^{*-5/2} + ...). \tag{16}$$

It states for large values of l_w or u_s which refer to large values of dimensionless distance, the migration velocity declines continuously. On a lighter note, as $d^* \to \infty$ migration velocity tends to be close to zero.
To sum up, the motion of a sphere immersed in a flow through a channel will be significantly decelerated because that sphere is affected by the walls.

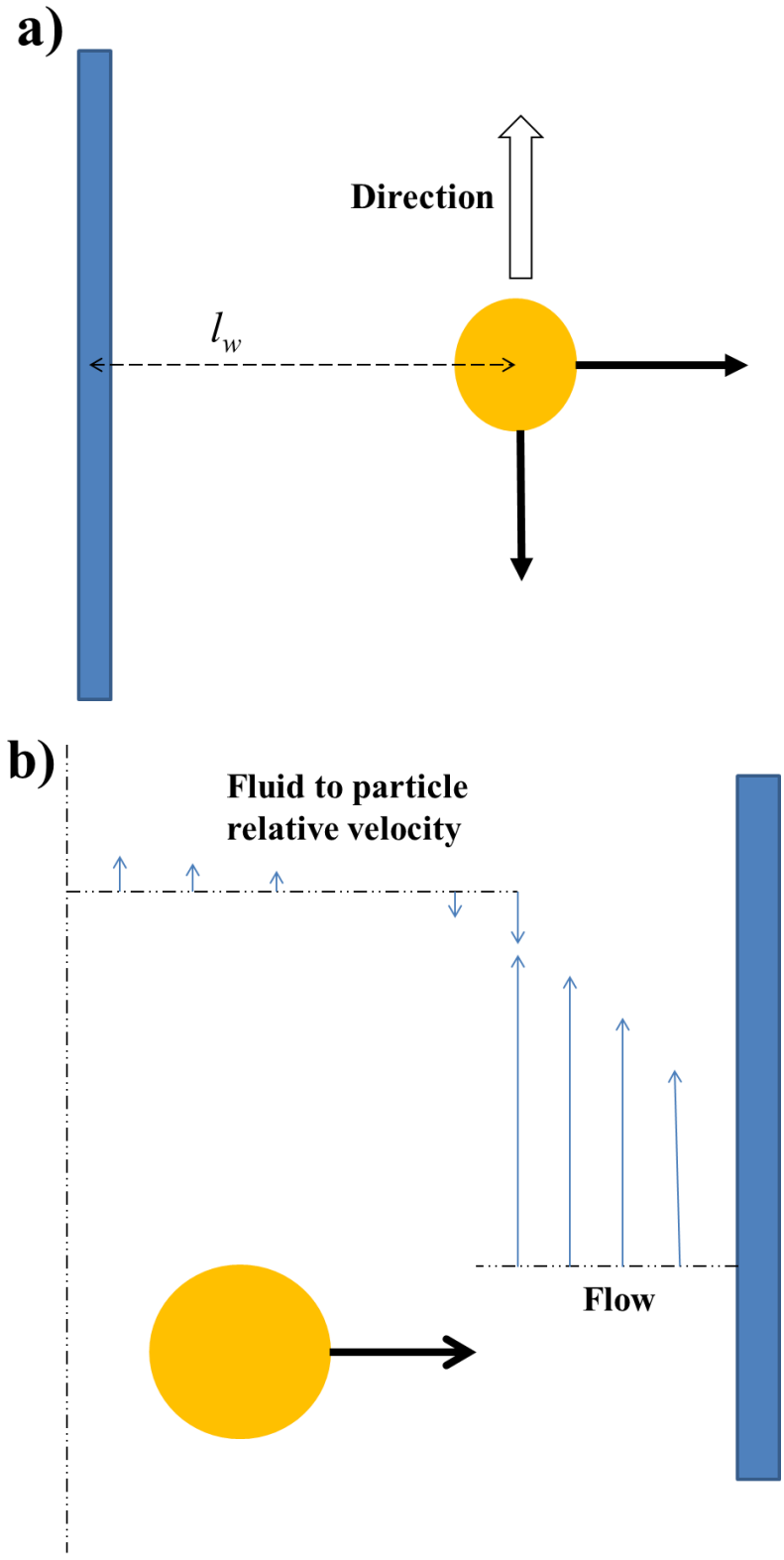

Figure 2. (a) The interaction of the ultrasmall particle and the small-scale channel (b) shear gradient lift force

Vector sum of lateral forces

While an immersed rigid sphere is flowing in Poiseuille flow in a straight channel, apart from viscous drag forces, four other types of force are applied perpendicular to the axis of the

channel. First of all, there is Magnus force which is induced by a pressure difference because of the streamline asymmetry as a result of the rotation of the sphere. Secondly, there is Saffman force induced by a fluid velocity gradient and its shear-induced particles rotation created by the wall effects. However these two forces are often considered negligible since they are very small [70]. Then, wall-induced and shear gradient lift forces are other two other forces which are considerable. As shear gradient lift force pushing the suspended particles toward to cannel walls, the wall-induced lift force directs particles toward to the channel centerline. These two push the particle towards the opposite sides until the balance of these forces forms some equilibrium positions between the channel centerline and the wall as observed by Serge and Silberberg [31, 71]. These positions are heavily dependent on the channel cross-sections.
An analytical formula of the overall lateral force on small particles was derived by Asmolov [72] using the method of matched asymptotic expansions.
If $d/d_h \ll 1$ in a Poiseuille:

$$F_L = f_{lift}\gamma^2\rho_f d^4, \tag{17}$$

or

$$F_L = f_{lift}\frac{\rho_f U^2 d^4}{{d_h}^2}, \tag{18}$$

where d_h is defined as hydraulic diameter which can be varied according to different cross-sections of the channels, for circular channels d_h represents the circular cross section diameter or for rectangular channels d_h is expressed as:

$$d_h = \frac{2wh}{(w+h)}. \tag{19}$$

In order to define the lift coefficient f_{lift} two factors are contributing: i) Reynolds number Re ii) lateral position of particle x_{eq} (Figure 3) [69, 72]. If $f_{lift} = 0$, the lateral equilibrium position is the same as inertial equilibrium position. Since any deflection from the channel centerline is non-returnable the channel centerline where $x = 0$ should not be considered as a stable equilibrium position. As Reynolds number increases the lift coefficient decreases. Therefore it can be found that ${U}^2_f$ scales more strongly than inertial lift force [48]. Based on experimental results, recently, a scaling for lift coefficient is achieved:

$$f_{lift} \propto \frac{{d_h}^2}{d^2\sqrt{\mathrm{Re}}}, \tag{20}$$

However, as Reynolds number is less than 100 in microfluidics platforms, the lift coefficient is usually considered constant as $f_{Lift} = 0.5$ [32]. For $0.05 \le d/d_h \le 0.2$, the particle size should be taken into account because its size would cause disturbance. By taking the advantage of finite element simulation and considering the finite-size of immersed object Di Carlo et al. [62] derived the lift forces. These calculated forces are varied according to whether the lift force is near the channel centerline where the wall-induced forces are mainly weak or walls where the wall-induced forces are significant.
Lift force near the channel centerline scales as:

$$F_{lift} \propto \frac{\rho_f {U_f}^2 d^4}{{d_h}^2}. \tag{21}$$

Lift force near the channel walls scales as:

$$F_{lift} \propto \frac{\rho_f U_f^{\,2} d^6}{d_h^{\,2}}. \tag{22}$$

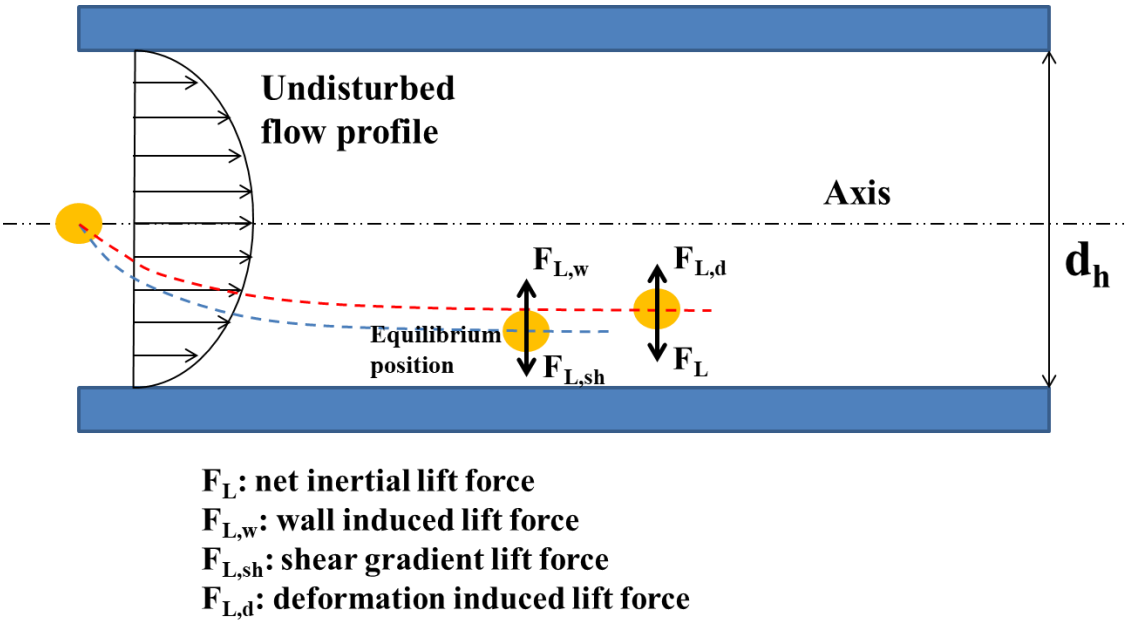

Figure 3. Various forces acting on an ultrasmall particle in a microfluidic channel.

Deformability-induced lift force

It is true that solid rigid spheres have being used as models in order to study hydrodynamic behavior of immersed objects in a microchannel. Practically, however, bio-particles are not rigid. Take cells and vesicles as good examples of these deformable bio-particles. Some additional lift forces will be induced because of this deformability. This deformability lift force which is at right angles to the channel centerline is widely thought to be resulted by shape-change of deformable particles. Matching velocities and stresses, moreover, produces nonlinearities at the interface of the deformable particles [73]. Apart from particle deformability, the shape of particles [27] and the properties of medium [74] could influence on lateral migration in a microchannel and equilibrium position. However we are not intended to discuss them here as the research on them is not well developed and they are often considered negligible.

Hur et al. [75]. Found that in the inertial microfluidics deformability-induced lift force which is directed to the channel centerline, thus, apparently pushes the particle more towards the centerline. Therefore the equilibrium positions formed by lift forces discussed above will be shifted a little closer to center of the microchannel. On a lighter note, the equilibrium positions created by deformable particles are somehow closer to the centerline than a solid particle. Circulating tumor cells (CTCs) are further deformable in comparison to the other cells. Therefore, they can be separated from circumferential blood by taking deformability and size into account.

For the sake of well recognizing the deformation of a droplet three dimensionless parameters should be considered:

1) Weber number

$$We = \frac{\rho_f U^2 d}{\sigma}, \tag{23}$$

where σ is the surface tension. Thus, Weber number accounts for inertial stress and surface tension

2) Capillary number

$$Ca = \frac{\mu U d}{\sigma h}. \tag{24}$$

Capillary number accounts for viscous stress and surface tension

3) Viscosity ratio:

$$\lambda_d = \frac{\mu_d}{\mu}, \tag{25}$$

where μ_d stands for the dynamic viscosity of fluid which is inside the droplet [73]. Deformability-induced lift force was analytically expressed by Chan and Leal when the drop or sometimes bubble is not in the vicinity of the walls [58, 76]:

$$F_{L,deformation} = \mu U d (\frac{d}{d_h})^2 \frac{d_c}{d_h} f(\lambda_d), \tag{26}$$

$$f(\lambda_d) = \frac{16\pi}{(\lambda_d + 1)^3} \left[\frac{11\lambda_d + 10}{140} (3\lambda_d^3 - \lambda_d + 8) + \frac{3}{14} \frac{19\lambda_d + 16}{3\lambda_d + 2} (2\lambda_d^2 - \lambda_d - 1) \right], \tag{27}$$

where the distance between centerline and drop is d_c. While the deformability-induced lift force is towards centerline of the microchannel the condition of $\lambda_d < 1 or \lambda_d > 10$ must be satisfied [76]. Di Carlo et al. [62] were able to derive an expression for inertial lift force based on empirically measuring of this force in the vicinity of the channel centerline.

If $\frac{d_c}{d_h} < 0.1$

$$F_{L,inertial}^{center} = -10 R_p \mu U d (\frac{d_c}{d_h}). \tag{28}$$

The negative sign stems from the centerline-directed nature of this inertial lift force. An equation for net lift force on bubbles or drops was experimentally extracted by Stan et al.[58] When inertial lift forces and drop deformation are small.

for $Ca < 0.01$ and $R_p < 0.01$

$$F_{L,empirical} = C_L \mu U d (\frac{d}{d_h})^3 (\frac{d_c}{d_h}). \tag{29}$$

Here C_L is lift coefficient. Although, for the sake of estimation $C_L \sim 31.25$ can be considered, generally, there are other empirical measurement methods too.[58].

Deformability-induced lift force can play an important role in diagnosis of malaria by separating and enriching red blood cells (iRBCs) from healthy red blood cells (hRBCs). As hRBCs are more deformable than iRBCs, the resultant equilibrium positions by hRBCs will be shifted to a position a bit closer to the channel centerline. Furthermore, iRBCs are more rigid because of the proteins released by parasite that caused the cross-linking of the spectrin

network to be triggered in phospholipid bilayer membrane of the iRBCs. Therefore iRBCs migrate towards the walls because of huge mechanical collisions and hydrodynamic interactions between RBCs in haematocrit blood. Thus, malaria iRBCs can be emptied and enriched designated outlets [77].

Inertial migration in curved channels

When a particle is suspended in a curved channel where the inertia is finite, two factors are contributing; inertial migration as well as secondary Dean flow. For a neutrally immersed particle centrifugal effects are almost negligible [78]. For the sake of a wide range of applications of precise positioning and focusing in separation and concentration we are in need of considering and investigating both inertial lift forces and Dean flow. Particle diameter, channel dimensions, aspect ratio, flow rate and radius of curvature are significant external parameters in order to investigate and control the focusing behavior of a suspended particle.

Fundamentals of inertial migration in a curving channel

While particles are suspended in curved channels, it can be assumed that inertial migration resulted by lift forces and secondary flow would be superposed on immersed particles [32] (Figure 4). On a lighter note, particles in equilibrium positions are affected by a drag force and this drag force can even be totally proportional to U_D which is the local secondary flow field. Moreover, particles influenced by lift forces in equilibrium positions will be entrained by this "Dean drag" force which is at the right angles to the flow direction.
A ratio of forces discussed above was proposed which plays a key role in describing the behavior of particles flowing in channels [32, 79]. This inertial force ratio (inertial lift/Dean drag) is expressed as:

$$R_f = \frac{Rd^2}{H^3}, \tag{30}$$

where H and R are the smallest dimension of a channel and the largest radius of curvature in curved channels, respectively. In order to obtain the inertial force ratio, the dimensional scaling of inertial lift in the shear gradient area [62] should be divided by the scaling of Dean drag. Positions and changes related to Re are negligible. This dimensionless parameter is important in predicting particles behavior; if $R_f \to \infty$ and Reynolds number is sufficiently high, particle will be independent of the secondary flow and will migrate to the equilibrium positions. If $R_f \to 0$, the lift forces and equilibrium positions would be negligible. Therefore the particle will be entrained by the secondary flow. Finally, for intermediate R_f, the consequences of both inertial migration and secondary flow should be taken into account. According to recent experiments the intermediate range for R_f is defined as $R_f >\sim 0.04$ [55]. Therefore new focusing modes and applications will appear. As inertial force ratio depends on particle size various behavior can be demonstrated by the particles in curved channels. While smaller particle is entrained by the secondary flow, the larger one is migrated to the inertial equilibrium positions. It is undeniable that Dean drag and inertial lift forces have different values in various regions across the channel cross-section then this will be true for R_f. Therefore, there would be other factors underlying the behavior of two particles in almost the same size at two different positions across the channel cross-section. Thus, this could lead to continuous separations. It is true that analyzing particles behavior can be simplified by taking the advantage of inertial force ratio. However, precise understanding of location and

mechanism of superposition lift forces and secondary flow effects is difficult and almost remains both experimentally and theoretically unknown. Currently our understanding of the balance resulted by lift forces and secondary flow is heavily relied on Figure 4 [48].

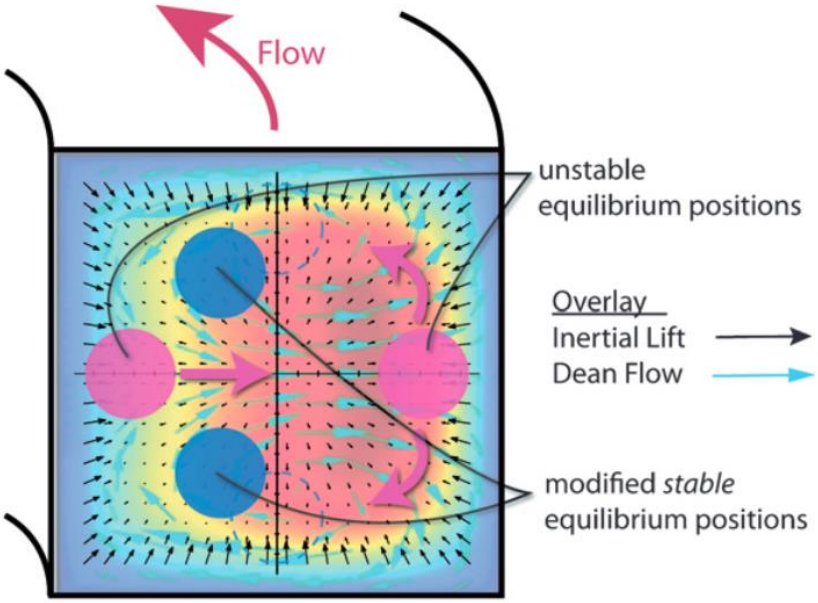

Figure 4. Dean flow and inertial lift directions in a curved channel; blue arrows: inertial lift force; green arrows: Dean flow velocity; blue dashed circles and red solid circles: the stable focusing locations of a straight channel [48] (reproduced with permission from the Royal Society of Chemistry).

Recent investigations on inertial microfluidics

Generally, with regard to channel structure, micro-channels can be divided into two category; straight channels and curved channels. The main difference between them is producing secondary flow resulted by channel curvature in curved channels which causes another dag force to appear. This force was comprehensively discussed above. In case of curved channels, there are different sorts of channels. Take spiral channel as a good example of curved channels which is widely applicable in disease diagnosis and biomedicine.

Recent progresses in inertial migration in straight micro-channels

In straight channels like other channel sorts, channel cross-section plays an important role in the equilibrium positions. If particles were randomly distributed in a micro-channel inlet that its cross-section is circular, particles would laterally migrate to an annulus-like position located at around 0.6 times of the radius of the channel from the axis [71, 80] (Figure 5a). Moreover, there are rectangular cross-section channels. They are mostly utilized because of their simplicity and convenience in fabricating. However, rectangular cross-section channels are more complex to be investigated rather than that of straight channels. Furthermore, the square channel, a rectangular straight channel when aspect ratio is one, provides four equilibrium positions for particles in front of the centers of all four walls [81] (Figure 5b). When aspect ratio is lower, in a rectangular straight channel, those equilibrium positions reduce to two ones at the center of two longer walls approximately 0.2 time of the H away from the walls (Figure 5c) [61].

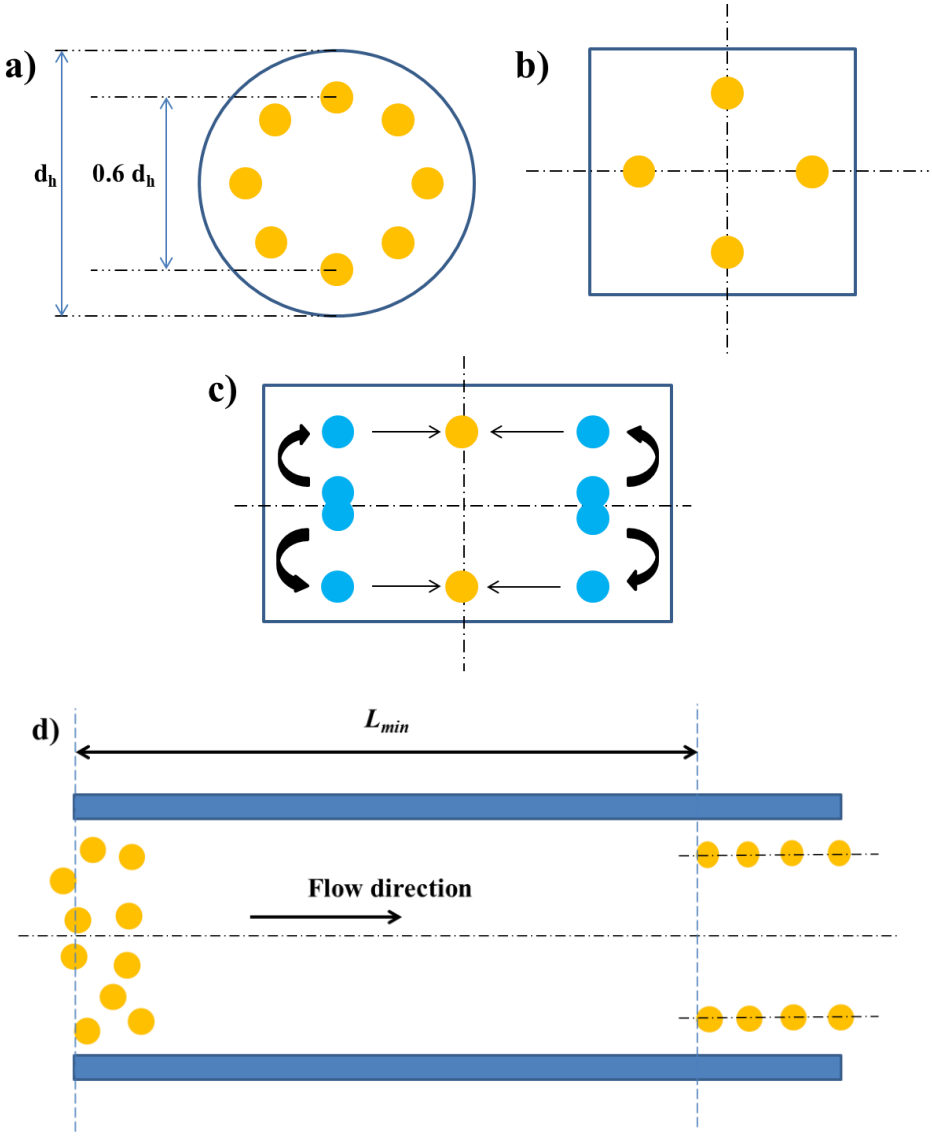

Figure 5. The inertial equilibrium state of straight microchannels with (a) circular, (b) square, and (c) rectangular cross-sectional shapes; (d) lateral migration phenomenon.

By balancing stokes drag force with net inertial lift force two significant parameters can be derived [69] (Figure 5d):

$$F_{stokes} = 3\mu\pi d U_L, \tag{31}$$

$$U_L = \frac{F_{Lift}}{3\mu\pi d} = \frac{\rho_f d^3 U_f^{\,2}}{6\mu\pi d_h^{\,2}}, \tag{32}$$

$$L_M \approx \frac{d_h}{2U_L} * U_f = \frac{3\mu_f d\pi d_h^{\,3}}{\rho_f U_f d^3}. \tag{33}$$

In order to characterize particles' lateral migration in a straight channel, channel Reynolds number Re and particle Reynolds number Rep can be used. The former describes the ratio between viscous and inertial forces caused by a fluid in a channel while the latter takes the ratio of the particle to channel dimensions into account. R_p can be derived as [32]:

$$R_p = \mathrm{Re}\frac{d^2}{d_h^2} = \frac{U_f \rho_f d^2}{\mu d_h}, \tag{34}$$

when $R_p \ll 1$, viscous drag forces are dominant then particles are influenced by them and follow the main streamline. On the other hand, when R_p is in the order of 1, inertial lift forces are dominant. Thus, particles will obviously migrate laterally [32].

The inertial migration of a particle/oblate spheroid was numerically studied in straight channels with rectangular and square cross-sections by Lashgary et al. [82]. They entirely analyzed migration dynamics of the oblate spheroid then compared the results to that of a sphere. The oblate particles usually migrate to one of the four equilibrium positions in a square channel which is similar to the inertial focusing of a rigid sphere. Furthermore, before reaching the equilibrium positions, an equilibrium manifold was observed by the lateral trajectories of oblate particles and spheres [82]. Apart from these similarities, there are differences between the migration of the spheres and oblates, too. Oblates tend to concentrate on the symmetry line of a channel cross-section which is diagonal and if their diameters are larger than a critical value, focusing particularly occurs in the vicinity of one of the corner. Moreover, the final rotation and orientation of the oblates was tumultuous when Reynolds number is larger than a certain threshold [82]. Finally it was documented in comparison with spherical particles the lateral migration of the oblates exhibit a less uniform behavior because of the obvious tumbling motion of the oblate particles throughout the migration [82].

An inertial microfluidic device was presented by Ming Li et al. [83] For continuous, passive, and high-throughput hydrogel droplets sorting by size. By taking the advantage of size-dependent equilibrium positions resulted by lateral migration this sorting is achieved; hydrogel droplets have different equilibrium positions due to their different sizes. Through this separation method smaller hydrogel droplets containing microalgal colonies are isolated from larger empty droplets [83].

This inertial microfluidic platform includes a straight rectangular microchannel, an inlet, a high aspect ratio (height/width>2) and a region gradually expanded into five different types of outlets. The fluid after these symmetric outlets will enter into fluidic resistors such as serpentine channels (Figure 6). In Figure 6a, it is showed how different-sized hydrogel droplets are located in three distinct regions while Reynolds number is finite. In the first region randomly distributed hydrogel droplets of different sizes are approaching to the inlet. Then, in the second region, two equilibrium positions are created along the long surfaces of the channel. These equilibrium positions appear because of the balance obtained between the wall-induced lift force and the shear-gradient lift force resulted in lateral migration. And smaller droplets migrate close to the sidewalls and larger ones to the centerline. While droplets arrived to the gradually expanded region, the equilibrium positions become distinctly separated. Eventually, different-sized hydrogel droplets would be emptied into fluidic resistors as the larger droplets are directed to the outlet designated along the channel centerline and the smallest ones are gathered from the closest outlet to the micro-channel walls [83].

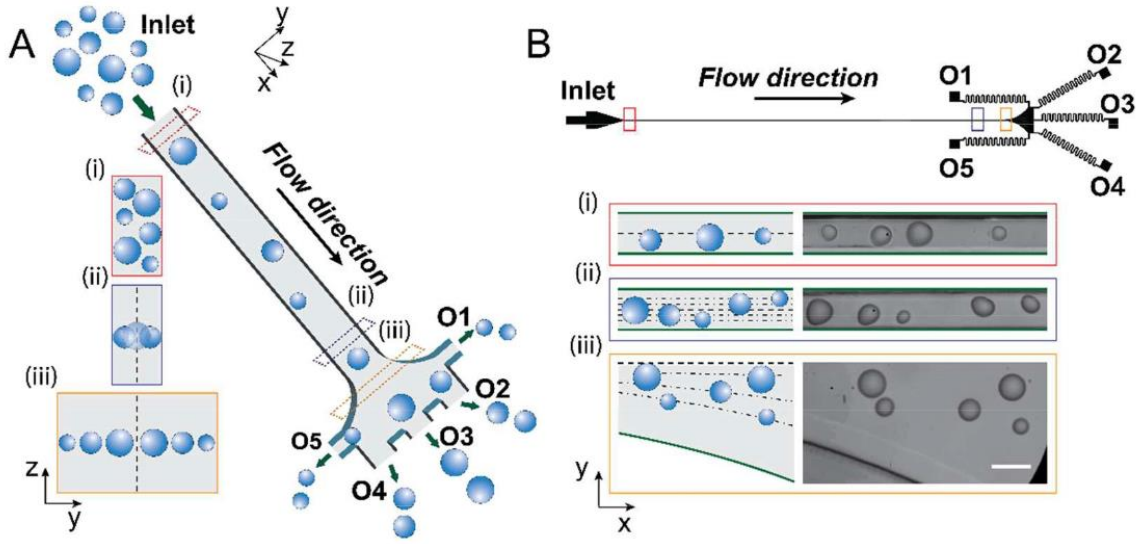

Figure 6. Hydrogel droplet separation (application of lateral inertial focusing): (a) separation procedure in an inertial microfluidics-based microchannel. (b) the top view of the microscale system [83] (reproduced with permission from the Royal Society of Chemistry).

In another investigation, Ming Li et al. [84] by using inertial microfluidics and a label-free, continuous, and high-throughput technique can separate E.gracilis by a shape parameter-cell aspect ratio. Euglena gracilis (E. gracilis) exhibits several shapes, for instance spindle-shaped, spherical, and elongated. An inertial microfluidic platform with a straight rectangular micro-channel, an inlet, a high aspect ratio (height/width>2) and a region gradually expanded into five outlets is used in the study. The fluid after these symmetric outlets will enter into fluidic resistors such as serpentine channels (Figure 7). E. gracilis cells' movement and position is indicated in three distinct regions: (i) randomly distributed E. gracilis cells are in the vicinity of the inlet; (ii) E. gracilis cells with different shapes influenced by two lift forces, laterally move to the equilibrium positions in front of the long channel surfaces. It is observed that the long rod-shaped cells' move closer to the channel centerline; (iii) by flowing along the streamline, some discrepancies in shape-dependent equilibrium positions will be more obvious (Figure 7a). Finally these separated cells are conducted into different outlets based on their positions; the longer rod-shaped cells are conducted into the outlet designated in the vicinity of the centerline and the spherical cells are directed to the outlets close to the channel sidewalls (Figure 7) [83, 84].

Inertial focusing phenomenon in a non-rectangular cross-section micro-channel was investigated by J. Kim et al. [85]. Purpose of the study was manipulating the flow velocity and the inertial focusing of micro-particles across the micro-channels. Focusing positions were analyzed in different Reynolds number and cross-sectional shapes for the sake of a comprehensive understanding of the exact situation and number of focusing positions. It is showed that when the symmetry of non-equilateral triangular channel cross-section is broken, the focusing positions will shift with varying Reynolds number [85]. A high purity in focusing (~99% purity) in a single stream achieved when channels with various cross-sections were connected [85].

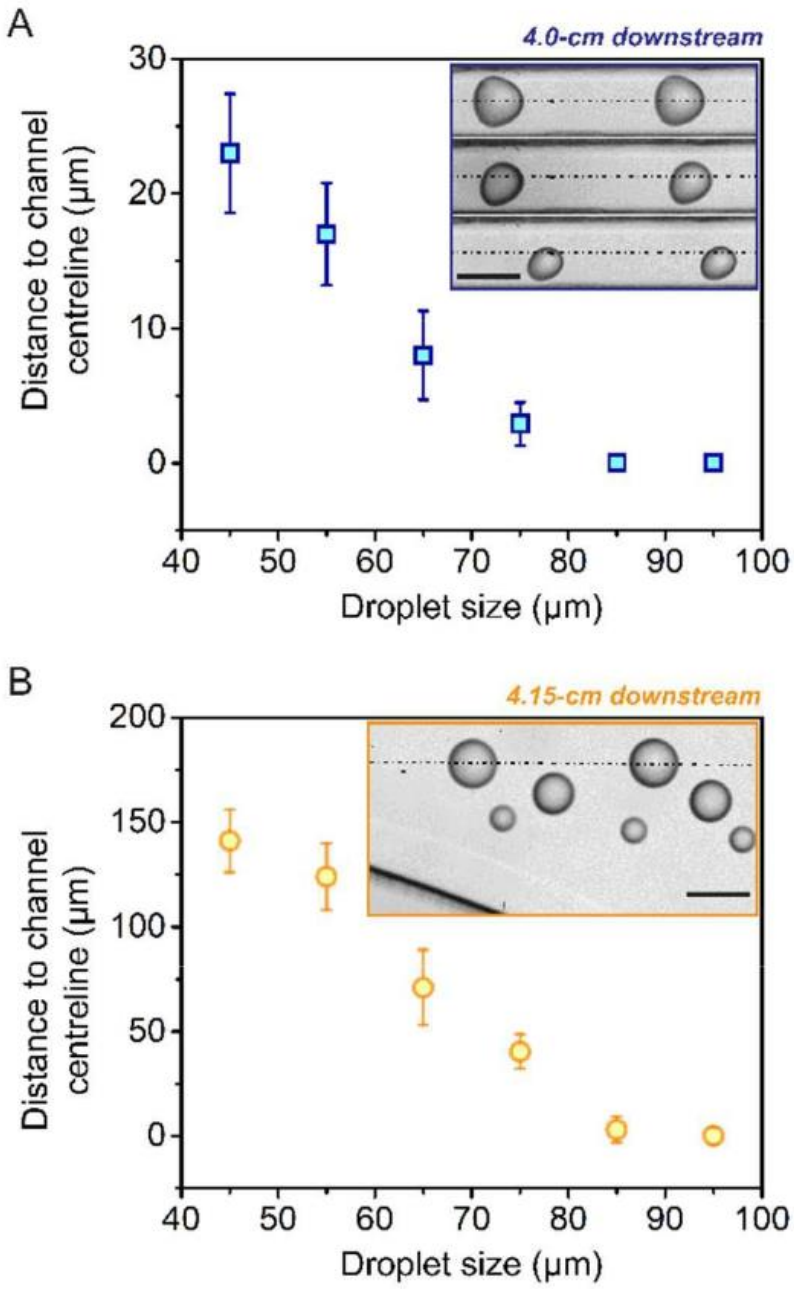

Figure 7. The mean distance to the microchannel center line for hydrogel droplets with various dimensions (Re = 55.7): (a) 4.0 cm entrance downstream: straight rectangular area; (b) 4.15 cm entrance downstream: expansion area [83] (reproduced with permission from the Royal Society of Chemistry).

To conclude, there are some unique advantages with straight channels such as its simplicity and ease of fabrication. Therefore, a wide variety of investigations have been done on this sort of channel structure. Thus, the migration in a straight micro-channel will be more simple and clearer than that of curved channel. According to $F_L \propto d_h^{-2}$, however, we have to restrict channel dimension to provide enough lateral forces. Moreover, flow resistance would be increased as this micro-channel length has to be relatively long. Therefore, although the mechanism of inertial focusing would be complex in a curved channel, we can take the advantage of the secondary flow produced by channel curvature to develop inertial migration and modify the equilibrium positions.

Recent progresses in inertial migration in spiral micro-channels

Now, curved channels will be discussed in this section. Thus, as previously mentioned, when a micro-channel is curved, the effects of secondary flow which is Dean drag force must be taken into account [70]. Curved channels are used in various structures; for instance spiral channels and serpentine channels. Spiral channels are presumably more applicable sort of curved channels [49]. Therefore, the research on them has been more developed. A spiral channel is formed by introducing curvature along a fixed axis.

Papautsky et al. [49] used spiral channels to separate 2 μm polystyrene particles from 7 μm ones. Furthermore, Seo et al. [86] used these channels for particle filtration. They can increase the size of the separation system to 100 L/min by cumulating disk-like filtration designs parallel [48]. Thus, their work is commercially well developed. This work is applicable in low maintenance, membrane-free, wastewater clarification, industrial liquid filtration and pre-treatment for desalination plants. It is showed that particles flowing in a curved channel with curvature radius of 20 mm spanning 180° are focused slightly away from the channel centerline in a streak and towards the outer wall. Interestingly, in this work in which square channels were used results were constant with that of a spiral channel with high aspect ratio where focusing occurs close to the internal wall [49, 86]. Thus, aspect ratio (W/H) plays a significant part in the distance between the internal wall and the focused streams in a curved channel as with increasing aspect ratio the focusing streams move insides. This is confirmed by Papautsky et al. [50] while k is constant, focusing streams moves towards the inner spiral channel wall as aspect ratio increases. Different-sized particles in spiral channels focused to various transverse locations across the channel cross-section according to small variations between the local ration of the lift force to Dean drag force. There is a privilege and a drawback with these approaches. The previously unexampled advantage is that different size particles in a single pass can be continuously separated while the drawback of applying spiral channels is the difficulty in placing many these systems on a single substrate to form a parallel system as the spiral channels turn in only one direction [48].

Another sort of particle separation was proposed by Yoon et al. [87]. They achieved the separation using overall outcomes of secondary flow speed distribution instead of balancing the inertial lift force influences and drag force caused by the secondary flow. Warkiani et al. [88] used a spiral system to achieve ≥85% recovery among several cancerous lines of cells and 99.99% WBCs depletions in whole blood. A confirmatory check using actual cancer cells lines was performed (Figure 8a) [88]. Device was characterized with cell samples to identify differences between the hydrodynamic behavior of the deformable cancer cells and rigid microbeads. To achieve this, the WBCs guided to an optimal platform then the cells distributing across the width of microchannel was observed (Figure 8b) [88]. In this work, the channel dimensions were optimized according to particle result. However, since an additional lift force is produced due to the interaction between deformable cells and fluid, the operational flow rate would be a little varied. Therefore, this additional lift force results in affecting equilibrium positions [88].

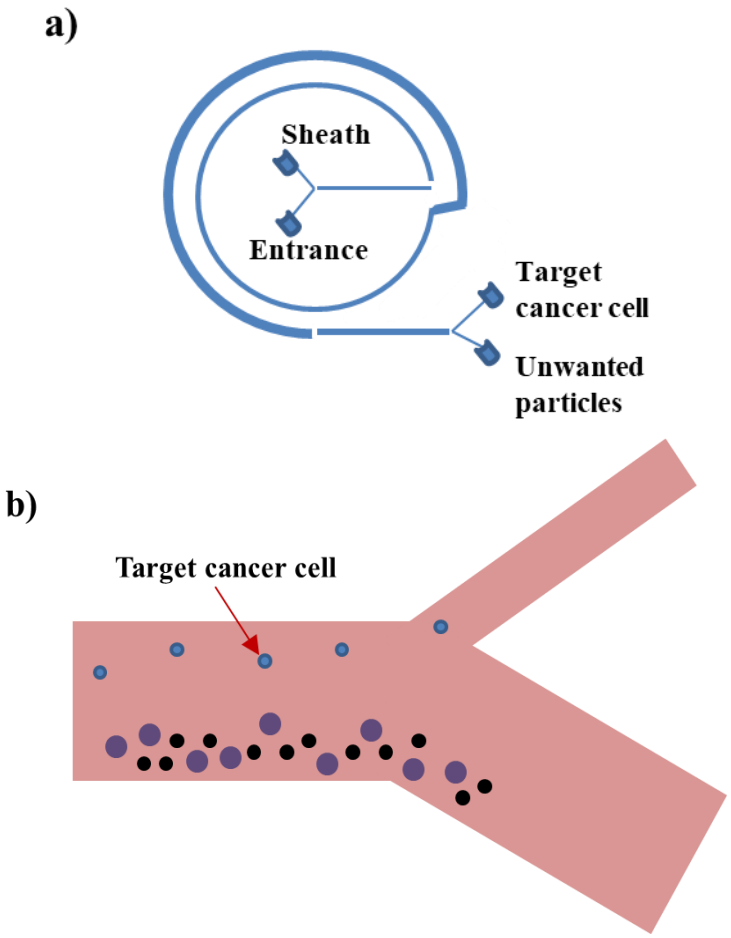

Figure 8. Spiral inertial microfluidic systems for circulating tumor cell separation; for more information, an interested reader can study the valuable work by Warkiani et al. [88].

Jeo-Ho Lee et al. [89] efficiently separated submicron-sized particles from larger particles by using net inertial force and Dean flow in a spiral microfluidic channel. When flow rate ratio is adjusted to the sheath flow at the inlet, smaller particles stream line circulating with Dean flow perpendicular to the mainstream will be distinguished from stream line of larger particles. Therefore, this separation is achievable [89].
A strategy was proposed by Nan Xiang et al. [90] to control the focusing position of particles in Dean-coupled elasto-inertial flows. When polymers are highly concentrated, particles flowing in a spiral microfluidic channel can be focused in a line precisely at the centerline of micro-channel where elastic forces are dominant [90]. This could be applicable in pretreatment process for micro-flow symmetry detection. As the polymer concentration decreases, the microparticles are shifted to the channel outer parts where there is a balance between elastic, net lift and Dean drag forces. Finally, Nan Xiang et al. [90] were able to employ the position-shifting for inertial focusing at higher throughputs compared to most other inertial elastic microfluidic platforms.

Recent progresses in inertial migration in serpentine micro-channels

In a spiral channel, distinctly, the curvature is designated along a single direction. Thus, after passing a certain channel length, the steady state flow would be achievable. This is almost regardless of various channel cross-sections. Through secondary flow-lift force combined techniques, particle behavior can be approximately analyzed. In serpentine channels,

nonetheless, the curvatures are alternating, thus, the situation gets more complex. For instance, the secondary flow would not achieve steady state after turning due to alternating curvatures. Therefore, particles behavior will be non-intuitive and unpredictable and analyzing the behavior of particles through the superposition technique is not reliable [70].
Effects of alternating curvatures on inertial migration of particles were investigated by Di Carlo et al. [32]. In their work, because of the symmetry, the four equilibrium positions in the straight channels would be reduced to just two positions in a microchannel of symmetric properties. Moreover, the equilibrium states are usually reduced more in an asymmetric serpentine channel to only one position. Therefore, focusing will be more sophisticated as Dean number increases (Figure 9). Based on their study, the balance between inertial lift load (F_L) and Dean drag load (F_D) plays an important role in determining most likely places of focusing locations. Although Dean flow is not contributing in creating inertial focusing, the flow can decrease the equilibrium position numbers formed by lift forces by acting combined with lift loads. When $F_D \ll F_L$, focusing will occur only because of inertial lift forces and when $F_D \gg F_L$, focusing will not occur since Dean flow is dominant. Then, the net lift-to-Dean drag ratios were:

$$\frac{F_L}{F_D} \sim R_e^n \frac{2R}{d_h}\left(\frac{d}{d_h}\right)^3, \quad (n<0) \tag{35}$$

At the constant Reynolds number, as FD is dominant for small particles, they will remain unfocused regardless of channel length. On the other hand, larger particles immediately become focused. Through applying this understanding, by using an asymmetric serpentine channel an inertial filtration device was successfully produced [79]. With regard to the fact that small particles remain unfocused and particles larger than a certain threshold can focus accordingly, large particles were totally eliminated from the mixture with a high purity (more than 90%). Nonetheless, small unfocused particles will enter the reservoir along with large particles. Therefore the purity rate in the collection of large particles is not acceptable.

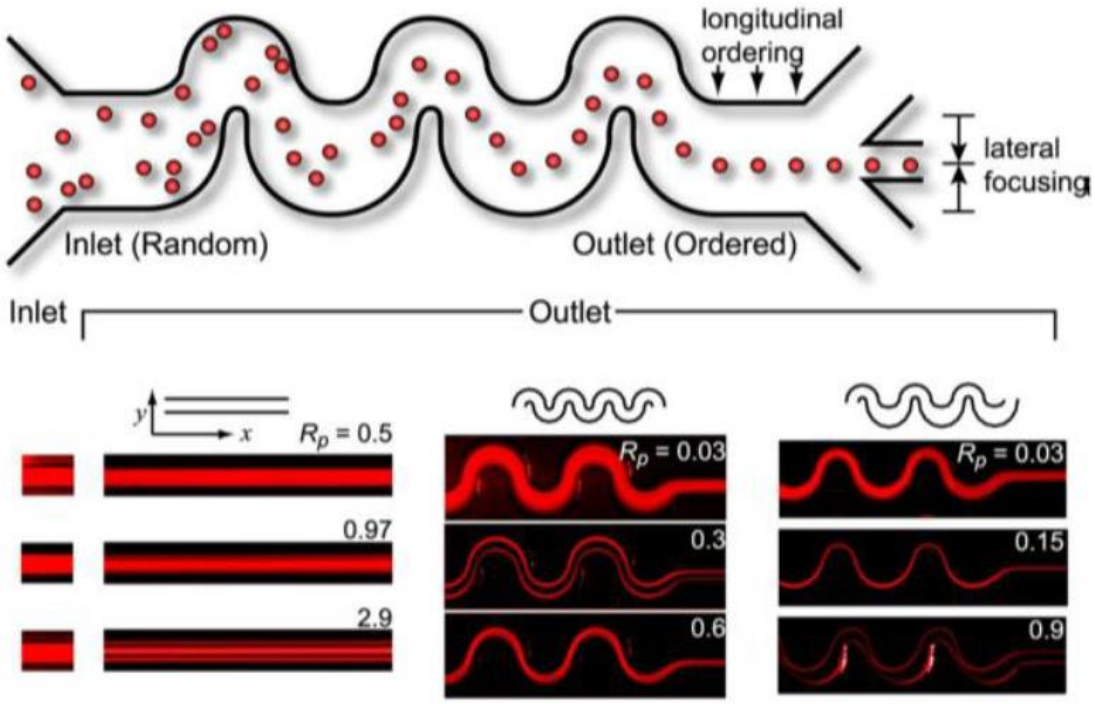

Figure 9. Self-ordering using an inertial microfluidics-based system; more details can be found in the interesting research work reported by Di Carlo et al. in Ref. [32] (reproduced with permission from PNAS).

A serpentine channel alternates turning direction and can be more easily parallelized. By the introduction of asymmetric curvature focusing like that of spiral channels is anticipated [32, 55]. Through parallel focusing ultra high-throughput flow cytometers will be achievable in which sheath fluids is not required. Therefore, an electrical or optical method will be employed that are sufficiently parallel. Applications in flow cytometry are encouraged by plenty of studies demonstrated high flow and shear rates do not have a significant impact on cells in an inertial microfluidics system since a cell cannot be located on surface stationaries while rotating and moving freely in a fluid, without deforming [32, 50, 79, 91]. On a lighter note, shear stress affection on cells are minimized when high shear rated are acting along with high rotation rates. Asymmetrically curved channels have been used for equilibrium separation. The fact that R_f is different for particles of different sizes is beneficial for selectively enriching larger particles at focusing positions in inertial microfluidics systems [79]. Platelets in diluted whole blood were selectively enriched over WBCs/RBCs by ~100-fold where the rate per channel was 1 mL/min.

The inertial focusing of particles simulation in 3D printed serpentine microfluidics was simulated practically studied [92]. Particles under an optimal condition were focused very well in the middle of the channel. Two types of cancer cells in this serpentine microfluidic channel, moreover, were focused under the optimal condition. This study can provide helpful insights into inertial focusing of particles simulating in 3D-printed microfluidics and promote this to commercial applications.

A high-throughput and continuous microfluidic WBCs separation platform was developed using particles differential inertial focusing in a serpentine channel [93]. The separation performance of this method was firstly characterized and evaluated by taking the advantage of a polystyrene bead in a serpentine microchannel. After two processes of cascading and when the average enrichment ratio was 28 times, 0.1% purity climbed to 80.3%. Then, to simulate WBCs flowing in whole blood, properties of particle separation and inertial focusing were investigated. WBCs were separated from Human whole blood then by the flow cytometry, WBCs purity separations were obtained. According to the results, it was proved that after two successive processes and when the average enrichment ratio was 10 times, WBC purity would be increased to 48%. Meanwhile, in order to achieve considerable fluid rates, a parallelized microfluidic platform was proposed.

Conclusions and prospective inertial microfluidics

While emerging decades ago, inertial microfluidics is recently becoming applicable. There still remain several latent aspects of this field to understand and develop related technologies. To improve future designs, disagreements between theoretical anticipations and experimental results should be identified. For instance, effects of particle shapes [32] and deformability-induced lift forces [94] can be more investigated to provide a better understanding for future modeling. Theoretical investigations will be required to achieve a wider insight into optimal separations designing of various particles and cells. This better understanding will be useful firstly in capturing more attention and audience who will be familiar with fundamentals of inertial effects in microfluidics. The more researchers will enter this area of science the more progresses will be made. Therefore, the currently overwhelmingly complex underlying theory behind these technologies can be well simplified in order to define design principles for practical models. Concisely, still more works should be done for the sake of an intuitive comprehension. In addition, for a wider understanding of microfluidics, apart from the channel structures presented in this paper that are relatively well studied so far now, there are still some other structures that still nascent and can be more investigated in the future. Palumbo et al.[95] used a helical channel, which is a relatively less studied channel structure,

for inertial particle separation to describe a microfluidic platform with a foot-print diameter of 5.5 mm.

There are a wide variety of problems in different subjects like biology and bioengineering expected to be solved by microfluidic approaches. For instance, microfluidic solutions are advantageous in providing technologies for diagnostics. However, as merely theoretical achievements like desired diagnostic devices are not able to be income generating the commercializing of these technologies will be a problem. Thus, making progress in academic research does not necessarily result in broad commercial markets. Having this said, a capable functionality by using microfluidics in comparison with current methods will play a vitally important role in developing the new methods which can stand a great chance of well commercializing.

Furthermore, looking for novel use of inertial microfluidics techniques can be of high promise. While inertial manipulation/focusing is useful in applications concerned with separations and flow cytometry, fluid movement by itself is applicable in mixing for Lab-on-a-Chip and opto-fluidics. Also, more investigation can be conducted to see whether it is possible to reduce sheath fluid reagent consumption in flow cytometry instrumentation by using inertial focusing or not. Additionally, according to massive parallelization new instruments can be made which will be beneficial in optical detection technologies. Separation without any membranes will be useful to explore in various applications like chemical and industrial processes, elusion processing and waste-water treatment. Interestingly, as biofuels are renewable they would mitigate the greenhouse gas emissions regardless of increasingly high energy demand due to economic growth. For example, biodiesel and bioethanol productions, driven from renewable sources, have recently gained much attention. But, there are several technical challenges such as separation and purification of microalgae from contaminants and harvesting of microalgae. Recently, it is showed that these challenges are surmountable using microfluidic devices [96]. However, there still remains a great need to make its applications commercially profitable. Finally, it is obvious it is not possible to list all of the prospective potential research areas pertaining to microfluidics while we have tried to refer to some ones expected to be more fruitful.

In summary, while considerable progress in inertial microfluidics has been made in recent decades even along with some commercially developed technologies, this area of science is still nascent and should be more and more explored and exploited. We believe inertial microfluidics will be as hot research topic in forthcoming future as it is now as well as its technological applications are expected to be expanded because superior advantages come with this science like simple structure, high throughput and low cost.

References

[1] Rad ER, Vahabi H, de Anda AR, Saeb MR, Thomas S. Bio-epoxy resins with inherent flame retardancy. Progress in Organic Coatings. 2019;135:608-12.

[2] Rohani Rad E, Vahabi H, Formela K, Saeb MR, Thomas S. Injectable poloxamer/graphene oxide hydrogels with well-controlled mechanical and rheological properties. Polymers for Advanced Technologies. 2019;30:2250-60.

[3] Vahabi H, Rad ER, Parpaite T, Langlois V, Saeb MR. Biodegradable polyester thin films and coatings in the line of fire: the time of polyhydroxyalkanoate (PHA)? Progress in Organic Coatings. 2019;133:85-9.

[4] Hadi A, Rastgoo A, Haghighipour N, Bolhassani A. Numerical modelling of a spheroid living cell membrane under hydrostatic pressure. Journal of Statistical Mechanics: Theory and Experiment. 2018;2018:083501.

[5] Barati A, Hadi A, Nejad MZ, Noroozi R. On vibration of bi-directional functionally graded nanobeams under magnetic field. Mechanics Based Design of Structures and Machines. 2020:1-18.
[6] Soleimani A, Dastani K, Hadi A, Naei MH. Effect of out-of-plane defects on the postbuckling behavior of graphene sheets based on nonlocal elasticity theory. Steel and Composite Structures. 2019;30:517-34.
[7] Nejad MZ, Hadi A, Farajpour A. Consistent couple-stress theory for free vibration analysis of Euler-Bernoulli nano-beams made of arbitrary bi-directional functionally graded materials. Structural engineering and mechanics: An international journal. 2017;63:161-9.
[8] Barreto JA, O'Malley W, Kubeil M, Graham B, Stephan H, Spiccia L. Nanomaterials: applications in cancer imaging and therapy. Advanced materials. 2011;23:H18-H40.
[9] Farajpour M, Shahidi A, Hadi A, Farajpour A. Influence of initial edge displacement on the nonlinear vibration, electrical and magnetic instabilities of magneto-electro-elastic nanofilms. Mechanics of Advanced Materials and Structures. 2019;26:1469-81.
[10] Asemi SR, Farajpour A, Borghei M, Hassani AH. Thermal effects on the stability of circular graphene sheets via nonlocal continuum mechanics. Latin American Journal of Solids and Structures. 2014;11:704-24.
[11] Asemi SR, Farajpour A. Vibration characteristics of double-piezoelectric-nanoplate-systems. Micro & Nano Letters. 2014;9:280-5.
[12] Safarabadi M, Mohammadi M, Farajpour A, Goodarzi M. Effect of surface energy on the vibration analysis of rotating nanobeam. 2015.
[13] Mohammadi M, Farajpour A, Goodarzi M, Heydarshenas R. Levy type solution for nonlocal thermo-mechanical vibration of orthotropic mono-layer graphene sheet embedded in an elastic medium. Journal of Solid Mechanics. 2013;5:116-32.
[14] Mohammadi M, Farajpour A, Goodarzi M, Dinari F. Thermo-mechanical vibration analysis of annular and circular graphene sheet embedded in an elastic medium. Latin American Journal of Solids and Structures. 2014;11:659-82.
[15] Farajpour MR, Shahidi AR, Farajpour A. Frequency behavior of ultrasmall sensors using vibrating SMA nanowire-reinforced sheets under a non-uniform biaxial preload. Materials Research Express. 2019;6:065047.
[16] Kordani N, Fereidoon A, Divsalar M, Farajpour A. Forced vibration of piezoelectric nanowires based on nonlocal elasticity theory. Journal of Computational Applied Mechanics. 2016;47:137-50.
[17] Whitesides GM. The origins and the future of microfluidics. nature. 2006;442:368-73.
[18] Farajpour M, Shahidi A, Farajpour A. Elastic waves in fluid-conveying carbon nanotubes under magneto-hygro-mechanical loads via a two-phase local/nonlocal mixture model. Materials Research Express. 2019;6:0850a8.
[19] Farajpour A, Żur KK, Kim J, Reddy J. Nonlinear frequency behaviour of magneto-electromechanical mass nanosensors using vibrating MEE nanoplates with multiple nanoparticles. Composite Structures. 2021;260:113458.
[20] Asemi S, Farajpour A, Mohammadi M. Nonlinear vibration analysis of piezoelectric nanoelectromechanical resonators based on nonlocal elasticity theory. Composite Structures. 2014;116:703-12.
[21] Gravesen P, Branebjerg J, Jensen OS. Microfluidics-a review. Journal of micromechanics and microengineering. 1993;3:168.
[22] Teh S-Y, Lin R, Hung L-H, Lee AP. Droplet microfluidics. Lab on a Chip. 2008;8:198-220.
[23] Bruus H. Theoretical microfluidics: Oxford university press Oxford, 2008.
[24] Hetsroni G, Mosyak A, Pogrebnyak E, Yarin L. Fluid flow in micro-channels. International Journal of Heat and Mass Transfer. 2005;48:1982-98.

[25] Martel JM, Toner M. Inertial focusing in microfluidics. Annual review of biomedical engineering. 2014;16:371-96.
[26] Karimi A, Yazdi S, Ardekani A. Hydrodynamic mechanisms of cell and particle trapping in microfluidics. Biomicrofluidics. 2013;7:021501.
[27] Hur SC, Choi S-E, Kwon S, Carlo DD. Inertial focusing of non-spherical microparticles. Applied Physics Letters. 2011;99:044101.
[28] Bhagat AAS, Bow H, Hou HW, Tan SJ, Han J, Lim CT. Microfluidics for cell separation. Medical & biological engineering & computing. 2010;48:999-1014.
[29] Weibel DB, Whitesides GM. Applications of microfluidics in chemical biology. Current opinion in chemical biology. 2006;10:584-91.
[30] Beebe DJ, Mensing GA, Walker GM. Physics and applications of microfluidics in biology. Annual review of biomedical engineering. 2002;4:261-86.
[31] Segre G, Silberberg A. Behaviour of macroscopic rigid spheres in Poiseuille flow Part 2. Experimental results and interpretation. Journal of fluid mechanics. 1962;14:136-57.
[32] Di Carlo D, Irimia D, Tompkins RG, Toner M. Continuous inertial focusing, ordering, and separation of particles in microchannels. Proceedings of the National Academy of Sciences. 2007;104:18892-7.
[33] Choi S, Park J-K. Continuous hydrophoretic separation and sizing of microparticles using slanted obstacles in a microchannel. Lab on a Chip. 2007;7:890-7.
[34] Choi S, Song S, Choi C, Park J-K. Hydrophoretic sorting of micrometer and submicrometer particles using anisotropic microfluidic obstacles. Analytical chemistry. 2009;81:50-5.
[35] Huh D, Bahng JH, Ling Y, Wei H-H, Kripfgans OD, Fowlkes JB, et al. Gravity-driven microfluidic particle sorting device with hydrodynamic separation amplification. Analytical chemistry. 2007;79:1369-76.
[36] Loutherback K, Chou KS, Newman J, Puchalla J, Austin RH, Sturm JC. Improved performance of deterministic lateral displacement arrays with triangular posts. Microfluidics and nanofluidics. 2010;9:1143-9.
[37] Wang X-B, Yang J, Huang Y, Vykoukal J, Becker FF, Gascoyne PR. Cell separation by dielectrophoretic field-flow-fractionation. Analytical chemistry. 2000;72:832-9.
[38] Messaud FA, Sanderson RD, Runyon JR, Otte T, Pasch H, Williams SKR. An overview on field-flow fractionation techniques and their applications in the separation and characterization of polymers. Progress in Polymer Science. 2009;34:351-68.
[39] Gossett DR, Weaver WM, Mach AJ, Hur SC, Tse HTK, Lee W, et al. Label-free cell separation and sorting in microfluidic systems. Analytical and bioanalytical chemistry. 2010;397:3249-67.
[40] McFaul SM, Lin BK, Ma H. Cell separation based on size and deformability using microfluidic funnel ratchets. Lab on a Chip. 2012;12:2369-76.
[41] Kralj JG, Lis MT, Schmidt MA, Jensen KF. Continuous dielectrophoretic size-based particle sorting. Analytical chemistry. 2006;78:5019-25.
[42] Zhu J, Tzeng TRJ, Xuan X. Continuous dielectrophoretic separation of particles in a spiral microchannel. Electrophoresis. 2010;31:1382-8.
[43] Voldman J. Electrical forces for microscale cell manipulation. Annu Rev Biomed Eng. 2006;8:425-54.
[44] Petersson F, Åberg L, Swärd-Nilsson A-M, Laurell T. Free flow acoustophoresis: microfluidic-based mode of particle and cell separation. Analytical chemistry. 2007;79:5117-23.
[45] Miltenyi S, Müller W, Weichel W, Radbruch A. High gradient magnetic cell separation with MACS. Cytometry: The Journal of the International Society for Analytical Cytology. 1990;11:231-8.

[46] Wang G, Yang F, Zhao W. There can be turbulence in microfluidics at low Reynolds number. Lab on a Chip. 2014;14:1452-8.
[47] Groisman A, Quake SR. A microfluidic rectifier: anisotropic flow resistance at low Reynolds numbers. Physical review letters. 2004;92:094501.
[48] Di Carlo D. Inertial microfluidics. Lab on a Chip. 2009;9:3038-46.
[49] Bhagat AAS, Kuntaegowdanahalli SS, Papautsky I. Continuous particle separation in spiral microchannels using dean flows and differential migration. Lab on a Chip. 2008;8:1906-14.
[50] Kuntaegowdanahalli SS, Bhagat AAS, Kumar G, Papautsky I. Inertial microfluidics for continuous particle separation in spiral microchannels. Lab on a Chip. 2009;9:2973-80.
[51] Rohani Rad E, Farajpour MR. Dynamics analysis of microparticles in inertial microfluidics for biomedical applications. Journal of Computational Applied Mechanics. 2019;50:157-64.
[52] Rohani Rad E, Farajpour MR. Influence of taxol and CNTs on the stability analysis of protein microtubules. Journal of Computational Applied Mechanics. 2019;50:140-7.
[53] Richardson JF, Harker JH, Backhurst JR. Particle technology and separation processes: Butterworth-Heinemann, 2002.
[54] Feng Z-G, Michaelides EE. Drag coefficients of viscous spheres at intermediate and high Reynolds numbers. J Fluids Eng. 2001;123:841-9.
[55] Gossett DR, Carlo DD. Particle focusing mechanisms in curving confined flows. Analytical chemistry. 2009;81:8459-65.
[56] Lu X, Liu C, Hu G, Xuan X. Particle manipulations in non-Newtonian microfluidics: A review. Journal of colloid and interface science. 2017;500:182-201.
[57] Elgeti J, Winkler RG, Gompper G. Physics of microswimmers—single particle motion and collective behavior: a review. Reports on progress in physics. 2015;78:056601.
[58] Stan CA, Ellerbee AK, Guglielmini L, Stone HA, Whitesides GM. The magnitude of lift forces acting on drops and bubbles in liquids flowing inside microchannels. Lab on a Chip. 2013;13:365-76.
[59] Liu C, Xue C, Sun J, Hu G. A generalized formula for inertial lift on a sphere in microchannels. Lab on a Chip. 2016;16:884-92.
[60] Longest PW, Kleinstreuer C, Buchanan JR. Efficient computation of micro-particle dynamics including wall effects. Computers & Fluids. 2004;33:577-601.
[61] Zhou J, Papautsky I. Fundamentals of inertial focusing in microchannels. Lab on a Chip. 2013;13:1121-32.
[62] Di Carlo D, Edd JF, Humphry KJ, Stone HA, Toner M. Particle segregation and dynamics in confined flows. Physical review letters. 2009;102:094503.
[63] Feng J, Hu HH, Joseph DD. Direct simulation of initial value problems for the motion of solid bodies in a Newtonian fluid. Part 2. Couette and Poiseuille flows. Journal of fluid mechanics. 1994;277:271-301.
[64] Matas J, Morris J, Guazzelli E. Lateral forces on a sphere. Oil & gas science and technology. 2004;59:59-70.
[65] Michaelides E. Particles, bubbles & drops: their motion, heat and mass transfer: World Scientific, 2006.
[66] Brenner H. The slow motion of a sphere through a viscous fluid towards a plane surface. Chemical engineering science. 1961;16:242-51.
[67] Cox R, Hsu S. The lateral migration of solid particles in a laminar flow near a plane. International Journal of Multiphase Flow. 1977;3:201-22.
[68] Vasseur P, Cox R. The lateral migration of spherical particles sedimenting in a stagnant bounded fluid. Journal of fluid mechanics. 1977;80:561-91.

[69] Bhagat AAS, Kuntaegowdanahalli SS, Papautsky I. Inertial microfluidics for continuous particle filtration and extraction. Microfluidics and nanofluidics. 2009;7:217-26.
[70] Zhang J, Yan S, Yuan D, Alici G, Nguyen N-T, Warkiani ME, et al. Fundamentals and applications of inertial microfluidics: a review. Lab on a Chip. 2016;16:10-34.
[71] Segre G, Silberberg A. Radial particle displacements in Poiseuille flow of suspensions. Nature. 1961;189:209-10.
[72] Asmolov ES. The inertial lift on a spherical particle in a plane Poiseuille flow at large channel Reynolds number. Journal of fluid mechanics. 1999;381:63-87.
[73] Amini H, Lee W, Di Carlo D. Inertial microfluidic physics. Lab on a Chip. 2014;14:2739-61.
[74] Lim EJ, Ober TJ, Edd JF, Desai SP, Neal D, Bong KW, et al. Inertio-elastic focusing of bioparticles in microchannels at high throughput. Nature communications. 2014;5:1-9.
[75] Hur SC, Henderson-MacLennan NK, McCabe ER, Di Carlo D. Deformability-based cell classification and enrichment using inertial microfluidics. Lab on a Chip. 2011;11:912-20.
[76] Chan P-H, Leal L. The motion of a deformable drop in a second-order fluid. Journal of fluid mechanics. 1979;92:131-70.
[77] Hou HW, Bhagat AAS, Chong AGL, Mao P, Tan KSW, Han J, et al. Deformability based cell margination—a simple microfluidic design for malaria-infected erythrocyte separation. Lab on a Chip. 2010;10:2605-13.
[78] Levesley J, Bellhouse B. Particulate separation using inertial lift forces. Chemical engineering science. 1993;48:3657-69.
[79] Di Carlo D, Edd JF, Irimia D, Tompkins RG, Toner M. Equilibrium separation and filtration of particles using differential inertial focusing. Analytical chemistry. 2008;80:2204-11.
[80] Matas J-P, Morris JF, Guazzelli É. Inertial migration of rigid spherical particles in Poiseuille flow. Journal of fluid mechanics. 2004;515:171-95.
[81] Choi Y-S, Seo K-W, Lee S-J. Lateral and cross-lateral focusing of spherical particles in a square microchannel. Lab on a Chip. 2011;11:460-5.
[82] Lashgari I, Ardekani MN, Banerjee I, Russom A, Brandt L. Inertial migration of spherical and oblate particles in straight ducts. Journal of fluid mechanics. 2017;819:540-61.
[83] Li M, van Zee M, Goda K, Di Carlo D. Size-based sorting of hydrogel droplets using inertial microfluidics. Lab on a Chip. 2018;18:2575-82.
[84] Li M, Muñoz HE, Goda K, Di Carlo D. Shape-based separation of microalga Euglena gracilis using inertial microfluidics. Scientific reports. 2017;7:1-8.
[85] Kim J-A, Lee J, Wu C, Nam S, Di Carlo D, Lee W. Inertial focusing in non-rectangular cross-section microchannels and manipulation of accessible focusing positions. Lab on a Chip. 2016;16:992-1001.
[86] Seo J, Lean MH, Kole A. Membrane-free microfiltration by asymmetric inertial migration. Applied Physics Letters. 2007;91:033901.
[87] Yoon DH, Ha JB, Bahk YK, Arakawa T, Shoji S, Go JS. Size-selective separation of micro beads by utilizing secondary flow in a curved rectangular microchannel. Lab on a Chip. 2009;9:87-90.
[88] Warkiani ME, Khoo BL, Wu L, Tay AKP, Bhagat AAS, Han J, et al. Ultra-fast, label-free isolation of circulating tumor cells from blood using spiral microfluidics. Nature protocols. 2016;11:134.
[89] Lee J-H, Lee S-K, Kim J-H, Park J-H. Separation of particles with bacterial size range using the control of sheath flow ratio in spiral microfluidic channel. Sensors and Actuators A: Physical. 2019;286:211-9.
[90] Xiang N, Ni Z, Yi H. Concentration-controlled particle focusing in spiral elasto-inertial microfluidic devices. Electrophoresis. 2018;39:417-24.

[91] Edd JF, Di Carlo D, Humphry KJ, Köster S, Irimia D, Weitz DA, et al. Controlled encapsulation of single-cells into monodisperse picolitre drops. Lab on a Chip. 2008;8:1262-4.
[92] Yin P, Zhao L, Chen Z, Jiao Z, Shi H, Hu B, et al. Simulation and practice of particle inertial focusing in 3D-printed serpentine microfluidics via commercial 3D-printers. Soft Matter. 2020.
[93] Zhang J, Yuan D, Sluyter R, Yan S, Zhao Q, Xia H, et al. High-throughput separation of white blood cells from whole blood using inertial microfluidics. IEEE transactions on biomedical circuits and systems. 2017;11:1422-30.
[94] Zhao Y, Sharp M. Finite element analysis of the lift on a slightly deformable and freely rotating and translating cylinder in two-dimensional channel flow. 1999.
[95] Palumbo J, Navi M, Tsai SS, Spelt JK, Papini M. Lab on a rod: Size-based particle separation and sorting in a helical channel. Biomicrofluidics. 2020;14:064104.
[96] Banerjee R, Kumar SJ, Mehendale N, Sevda S, Garlapati VK. Intervention of microfluidics in biofuel and bioenergy sectors: Technological considerations and future prospects. Renewable and Sustainable Energy Reviews. 2019;101:548-58.